International Journal of Thermophysics, Vol. 24, No. 4, July 2003 (© 2003)

Measurement of the Thermal Diffusivity of Solids with an Improved Accuracy

C. D. Martinsons,[1–3] A. P. Levick,[1] and G. J. Edwards[1]

Received August 15, 2002

A photothermal radiometry technique is being developed at the NPL with the goal of improving the accuracy of thermal diffusivity measurements. The principle is to perform a laser-induced thermal experiment while simultaneously making accurate measurements of the experimental boundary conditions. A numerical three-dimensional heat diffusion model based on thermal transfer functions has been developed to account for the measured boundary conditions. The thermal diffusivity is determined from the experimental data by a nonlinear, least-squares fit to the model. Experiments carried out on pure metals at 900 K demonstrate good agreement between the theoretical predictions and experimental data, and uncertainties of about 1.5% for the thermal diffusivities of platinum, titanium, and germanium were obtained.

KEY WORDS: germanium; infrared; laser; optical techniques; photothermal radiometry; platinum; thermal diffusivity; titanium.

1. INTRODUCTION

Photothermal techniques are being developed at the NPL for the simultaneous measurement of temperature [1] and thermophysical properties such as emissivity, thermal diffusivity, and thermal conductivity. This paper describes the results of recent investigations directed particularly at improving the accuracy of thermal diffusivity measurements. Well-established techniques for the determination of the thermal diffusivity of solids

[1] Centre for Basic, Thermal and Length Metrology, National Physical Laboratory, Teddington, Middlesex, TW11 0LW, United Kingdom.
[2] Present address: ATRAL S.A., Rue du Pre de l'Orme, 38926 Crolles Cedex, France.
[3] To whom correspondence should be addressed. E-mail: lynnmartinsons@free.fr

0195-928X/03/0700-1171/0 © 2003 Plenum Publishing Corporation

such as the flash technique [2, 3] or thermal wave techniques [4] often rely on simplified geometries and ideal boundary conditions used *a priori* in a mathematical model. Systematic errors inevitably occur because of experimental deviations from initial assumptions [4]. In the most widely used technique, the laser-flash technique, a uniform one-dimensional excitation and a simple temporal pulse shape are assumed [2, 3]. Pulsed laser beams are in essence difficult to measure, and the desired characteristics are not always met. This may partly explain why the uncertainties reported for thermal diffusivity values are rarely better than a few percent, even with high purity materials.

We propose a new methodology, based on photothermal infrared radiometry [5], to measure the thermal diffusivity of materials with better accuracy. The principle is to detect a laser-induced thermal radiance signal while simultaneously making accurate measurements of the boundary conditions of the heat conduction problem. In the case of a sufficiently large sample opaque at the pump wavelength, the only boundary conditions are the laser beam profile at the surface and the time dependence of the incident intensity.

The excitation of the sample is achieved using a periodically scanned continuous-wave laser beam. By absorption of a fraction of the incident light, a periodic temperature field is induced which, in turn, is responsible for a modulation of the thermal radiance emitted by the stimulated surface. Visible and infrared optical detection is performed in the time domain to measure the modulated thermal radiance and the back-scattered laser light. The modulated thermal radiance is proportional to a local average of the induced temperature field whereas the back-scattered signal gives the time dependence of the incident laser intensity. The beam profile is accurately measured using a beam-analyzing device consisting of a scanning slit attached to the moving mirror of a Michelson interferometer. The experimental setup is more precisely described in Section 2.

The theoretical waveform of the periodic temperature field is given by a linear relationship between the thermal source term and a heat diffusion operator. Fourier analysis of the heat conduction problem shows that the latter behaves as a low-pass filter whose cut-off frequency depends on the thermal diffusivity. Section 3 presents the mathematical model used to solve this three-dimensional time-dependent heat conduction problem.

The thermal diffusivity is determined from the experimental data sets by a nonlinear least-squares fit to the model. The algorithm is presented in Section 4.

Experimental data on platinum, titanium, germanium, and copper heated to 900 K in air are presented and discussed in Section 5.

2. EXPERIMENTAL SETUP

A schematic of the photothermal setup is shown in Fig. 1. The sample's front surface is optically excited by an argon ion laser beam delivering a maximum power of 2 W at 514.5 nm. A laser scanner, driven by a programmable function generator, is used to periodically scan the beam across the sample surface. A CaF_2 plano-convex doublet forms an image of a fixed point of the surface onto two optical detectors. The doublet is used in 1 to 1 imaging ratio and has a numerical aperture of about 0.1. The optical signal is the superimposition of the back-scattered laser light and the thermal radiance emitted by the sample surface. A long-wave-pass germanium beamsplitter is used to transmit wavelengths greater than 1.85 μm towards an InSb infrared detector (dimensions 0.1 mm × 0.1 mm) and to reflect shorter wavelengths towards a silicon detector which has a suppressed infrared sensitivity. The infrared thermal radiance is filtered using a narrow bandwidth interference filter centred at 4.05 μm. A narrow bandwidth detection has the advantage of minimizing the effect of chromatic aberrations induced by the collecting lenses.

When a square wave is used to drive the scanner, the beam is periodically deflected on and off the targeted spot, producing a chopped laser excitation. Unlike an optical chopper, the laser scanner can be operated reproducibly at very low frequencies with a short time step (< 10 μs).

After preamplification, both the back-scattered signal and the thermal radiance signal are digitized using a 16 bit A/D card. The data acquisition

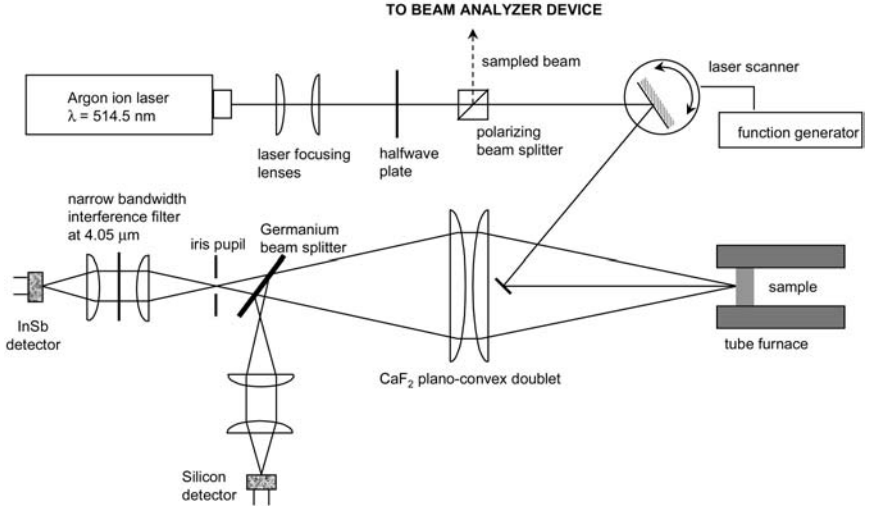

Fig. 1. Photothermal radiometry setup.

is triggered by a 100 kHz clock signal generated by a frequency multiplier from the low-frequency signal that drives the laser scanner. This synchronous sampling allows averaging of the signal over a great number of periods without significant drift or waveform distortion. The averaging process is realized in real time by an infinite impulse response digital filter implemented with LabView. The laser scanner driving signal is usually a 10 Hz square wave, and typically the sampled sets of back-scattered and thermal radiance data consist of $N = 10000$ points.

During this data acquisition, a small fraction of the excitation laser beam is sampled using a polarizing beamsplitter cube and sent to a beam analyzing device. In order to measure the beam profile at the position of the sample surface, the beamsplitter is placed at identical optical path lengths from the sample and the beam analyzer.

The beam analyzer (Fig. 2) is a scanning slit whose displacement is monitored by a Michelson interferometer. A large area silicon photodiode placed behind a 10 μm wide slit is mounted on a motorized translation stage together with one of the interferometer mirrors. Using a 5 mW HeNe laser source, the movement of the assembly produces highly contrasted sinusoidal interference fringes which are detected by another silicon photodiode. Each fringe corresponds to a displacement equal to half a wavelength of the HeNe laser, i.e., $\Delta x = 0.3164$ μm. An electronic trigger circuit generates a reference TTL signal from the fringe signal. Both the reference

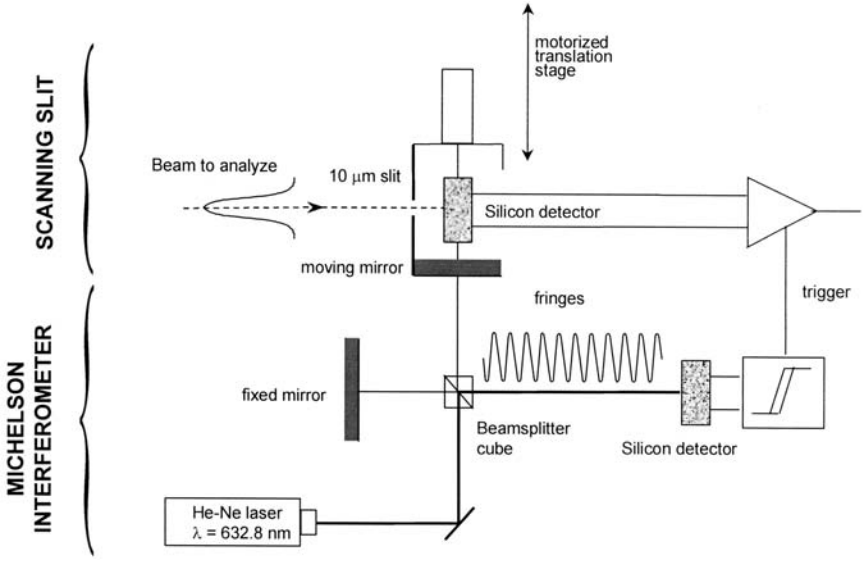

Fig. 2. Beam analyzer device.

signal and the scanning slit signal are fed in an A/D card, and a LabView program is used to acquire one sample for every 10 fringes detected, equivalent to a slit displacement of 3.164 μm. The accuracy of the beam profile measurement is assessed by fitting a Gaussian profile to the data. The uncertainty on the beam diameter is typically 0.2%.

3. MATHEMATICAL MODELING

With a laser spot with a diameter of about 2 mm and a scanning frequency greater than a few tenths of Hertz, the thermal perturbation is confined within a volume of about 1 mm^3 for most materials. Therefore, the heat conduction problem solved for a semi-infinite medium is appropriate.

Let us assume a periodically modulated laser beam incident on the surface of an opaque semi-infinite homogeneous material. The absorbed laser light is converted into heat which diffuses in the material. In the case of a chopped-like modulation, the source term of the thermal problem can be expressed as the product of a spatial term and a temporal term:

$$q(x, y, z, t) = f(x, y)\, \delta(z)\, h(t) \tag{1}$$

where $f(x,y)$ is the beam profile, δ is the Dirac distribution, and $h(t)$ is the time dependence of the laser intensity. The temperature field $T(x, y, z, t)$ in the material is the solution of the three-dimensional heat conduction problem defined by the following differential system [6]:

$$\nabla^2 T = \frac{1}{D}\frac{\partial T}{\partial t} \tag{2a}$$

$$T(x, y, z, t)]_{t=0} = 0 \tag{2b}$$

$$K \frac{\partial T}{\partial z}\Bigg]_{z=0} = -q(x, y, z, t) \tag{2c}$$

$$T(x, y, z, t)]_{z\to\infty} = 0 \tag{2d}$$

$$T(x, y, z, t)]_{x\to\infty} = 0 \quad \text{and} \quad \frac{\partial T(x, y, z, t)}{\partial x}\Bigg]_{x\to\infty} = 0 \tag{2e}$$

$$T(x, y, z, t)]_{y\to\infty} = 0 \quad \text{and} \quad \frac{\partial T(x, y, z, t)}{\partial y}\Bigg]_{y\to\infty} = 0 \tag{2f}$$

K and D are, respectively, the thermal conductivity and the thermal diffusivity of the material. $h(t)$, a periodic function with a frequency γ, can be expanded in a Fourier series:

$$h(t) = \sum_{n=-\infty}^{n=+\infty} \tilde{h}_n e^{2i\pi n\gamma t} \tag{3}$$

where $\tilde{h}_n$ is the nth component of the Fourier spectrum of $h(t)$. After a transient regime, a periodic regime is established in the material. The temperature field can therefore be Fourier expanded:

$$T(x, y, z, t) = \sum_{n=-\infty}^{n=+\infty} \tilde{T}_n(x, y, z)\, e^{2i\pi n\gamma t} \tag{4}$$

The terms $\tilde{T}_n$ are the components of the Fourier spectrum of $T(x, y, z, t)$. Replacing T by its Fourier expansion in Eqs. (2) leads to a differential system for each component $\tilde{T}_n$:

$$\nabla^2 \tilde{T}_n = \frac{2i\pi n\gamma}{D} \tilde{T}_n \tag{5a}$$

$$K \frac{\partial \tilde{T}_n}{\partial z}\Bigg]_{z=0} = -f(x, y)\, \tilde{h}_n \tag{5b}$$

$$\tilde{T}_n(x, y, z)]_{z\to\infty} = 0 \tag{5c}$$

$$\tilde{T}_n(x, y, z)]_{x\to\infty} = 0 \qquad \text{and} \qquad \frac{\partial \tilde{T}_n}{\partial x}\Bigg]_{x\to\infty} = 0 \tag{5d}$$

$$\tilde{T}_n(x, y, z)]_{y\to\infty} = 0 \qquad \text{and} \qquad \frac{\partial \tilde{T}_n}{\partial y}\Bigg]_{y\to\infty} = 0 \tag{5e}$$

Let $\tilde{v}_n(u_x, u_y, z)$ be the two-dimensional spatial Fourier transform of $\tilde{T}_n(x, y, z)$ with respect to x and y:

$$\tilde{v}_n(u_x, u_y, z) = \int_{-\infty}^{+\infty} \int_{-\infty}^{+\infty} \tilde{T}_n(x, y, z)\, e^{-2i\pi(u_x x + u_y y)}\, dx\, dy \tag{6}$$

The spatial frequencies u_x and u_y form a continuum in the real space because of the unbounded conditions, Eqs. (5d) and (5e) [7]. Replacing $\tilde{T}_n$ by its Fourier decomposition leads to a one-dimensional differential system for $\tilde{v}_n$ as a function of the space variable z:

$$[(2i\pi u_x^2)+(2i\pi u_y^2)]\,\tilde{v}_n+\frac{d^2\tilde{v}_n}{dz^2}=\frac{2i\pi\gamma}{D}\,\tilde{v}_n \tag{7a}$$

$$K\frac{d\tilde{v}_n}{dz}\Bigg]_{z=0}=-\tilde{f}(u_x, u_y)\,\tilde{h}_n \tag{7b}$$

$$\tilde{v}_n(u_x, u_y, z)]_{z\to\infty}=0 \tag{7c}$$

where $\tilde{f}(u_x, u_y)$ is the Fourier transform of the beam profile.

The solution of the differential system defined by Eqs. (7), expressed at $z=0$, is

$$\tilde{v}_n(u_x, u_y, z)=\frac{\sqrt{D}}{K}\frac{\tilde{f}(u_x, u_y)\,\tilde{h}_n}{\sqrt{2i\pi n\gamma+4\pi^2D(u_x^2+u_y^2)}} \tag{8}$$

Equation (8) shows that the surface temperature in the Fourier domain is the algebraic product of the beam profile Fourier component $\tilde{f}(u_x, u_y)$ by the Fourier component of the laser intensity time dependence $\tilde{h}_n$ and by a thermal transfer function $H_n(u_x, u_y)$ defined by

$$H_n(u_x, u_y)=\frac{\sqrt{D}}{K}\frac{1}{\sqrt{2i\pi n\gamma+4\pi^2D(u_x^2+u_y^2)}} \tag{9}$$

The surface temperature field in the Fourier domain can be seen as the result of a linear filter H acting on two input functions $\tilde{f}$ and $\tilde{h}_n$:

$$\tilde{v}_n(u_x, u_y, z=0)=H_n(u_x, u_y)\,\tilde{f}(u_x, u_y)\,\tilde{h}_n \tag{10}$$

In the experimental setup, a photodetector of dimensions x_d and y_d is used to detect the thermal radiance emitted by the surface in a small spectral band centred around the detection wavelength. In the limit of small laser heating, the signal $S(t)$ induced by the laser periodic heating is proportional to the periodic surface temperature, averaged on the detection zone. The proportionality factor, which includes the local emissivity, the first derivative of the Planck function, the numerical aperture of the optics, and the instrumental gain, is omitted for clarity:

$$S(t)=\frac{1}{x_d\,y_d}\int_{-x_d/2}^{x_d/2}\int_{-y_d/2}^{y_d/2}T(x, y, z=0, t)\,dx\,dy \tag{11}$$

$S(t)$ is also a periodic function and, therefore, can be expressed as a Fourier series with coefficients $\tilde{S}_n$. According to Eq. (11), $\tilde{S}_n$ is given by

$$\tilde{S}_n=\frac{1}{x_d\,y_d}\int_{-x_d/2}^{x_d/2}\int_{-y_d/2}^{y_d/2}\tilde{T}_n(x, y, z=0)\,dx\,dy \tag{12}$$

After replacing $\tilde{T}_n$ by its two-dimensional Fourier expansion and performing the double integration over x and y, Eq. (12) becomes

$$\tilde{S}_n = \int_{-\infty}^{+\infty} \int_{+\infty}^{+\infty} \tilde{v}_n(u_x, u_y, z = 0)\, \mathrm{sinc}(\pi x_d u_x)\, \mathrm{sinc}(\pi y_d u_y)\, du_x\, du_y \quad (13)$$

where $\mathrm{sinc}(x) = \sin(x)/x$. Let us define the detector transfer function $T(u_x, u_y)$:

$$T(u_x, u_y) = \mathrm{sinc}(\pi x_d u_x)\, \mathrm{sinc}(\pi y_d u_y) \quad (14)$$

The Fourier components $\tilde{S}_n$ of the periodic signal can now be expressed as

$$\tilde{S}_n = \tilde{h}_n \int_{-\infty}^{+\infty} \int_{+\infty}^{+\infty} H_n(u_x, u_y)\, T(u_x, u_y)\, \tilde{f}(u_x, u_y)\, du_x\, du_y \quad (15)$$

Assuming a rotational symmetry of the laser beam, Eq. (15) becomes

$$\tilde{S}_n = \tilde{h}_n \int_{-\infty}^{+\infty} \int_{-\infty}^{+\infty} H_n(u_x, u_y)\, T(u_x, u_y)\, \tilde{f}(u_x)\, \tilde{f}(u_y)\, du_x\, du_y \quad (16)$$

The periodic signal $S(t)$ is given by the following Fourier series:

$$S(t) = \sum_{n=-\infty}^{\infty +} \tilde{S}_n e^{2i\pi n y t} \quad (17)$$

The numerical implementation of the model was done using MATLAB. The Fourier spectra $\tilde{f}$ and $\tilde{h}_n$ are computed using the fast Fourier transform algorithm (FFT) applied to the beam profile and the backscattered light data. The double integral in Eq. (16) is approximated by a double sum over the positive spatial frequencies. $S(t)$ is computed according to Eq. (17) by inverse FFT. The computation of a set of 10000 values of $S(t)$ takes about 10 s on a 350 MHz PC.

3. PARAMETER ESTIMATION AND MEASUREMENT UNCERTAINTY

Although the temperature and the photothermal signal are given by linear relationships, the model described in Section 2 is not linear with respect to the thermal diffusivity. This parameter must be therefore determined by a nonlinear parameter estimation procedure aiming to fit the model to the thermal radiance data. Assuming Gaussian white noise with zero-mean and uniform variance, the least-squares technique provides

minimal variance estimators [8]. In order to avoid any bias, the experimental data are not normalized. Instead, instrumental parameters (offset, gain, and arbitrary time origin) are estimated together with the diffusivity in the form of a four-parameter vector $\mathbf{m}^t = (D, \text{offset}, \text{gain}, \text{origin})$. The Gauss–Newton iterative algorithm is chosen to perform the minimization of the least-squares cost function. In this technique, the first partial derivatives of the model with respect to the parameters are needed to compute the $N \times 4$ Jacobian matrix G of the problem:

$$G_{ij} = \left(\frac{\partial S(t)}{\partial m_j} \right)_{t = t_i} \tag{18}$$

The partial derivative with respect to the diffusivity is approximated by a finite-difference technique. Since the data depend linearly on the instrumental parameters, the computation of the corresponding partial derivatives is straightforward [8].

This parameter estimation problem is well-conditioned and the algorithm usually converges after 3 or 4 iterations when realistic initial values are used. An estimate $\hat{\sigma}^2$ of the variance of the noise is given by:

$$\hat{\sigma}^2 = \frac{1}{N-4} \sum_{i=1}^{N} (S_{\text{exp}}(t_i) - S_{\text{theo}}(t_i))^2 \tag{19}$$

where $S_{\text{exp}}(t_i)$ and $S_{\text{theo}}(t_i)$ are, respectively, the measured and the fitted theoretical data.

There are three contributions to the uncertainty of the estimated parameters: the noise in the thermal radiance data, the error in the measurement of the beam profile, and the error in the measurement of the laser intensity time dependence. Because of the very good accuracy in the measurements of the beam profile and the laser intensity time dependence, their contributions are negligible compared to the thermal radiance noise, which is essentially due to the background photon noise. The uncertainty of the estimated parameters is therefore derived from the fitting residuals only. The covariance matrix $C_{\mathbf{m}}$ of the estimated parameters is computed using the linear least-squares theory:

$$C_{\mathbf{m}} = \hat{\sigma}^2 (G^t G)^{-1} \tag{20}$$

where G is evaluated using the optimal values of the parameters. The thermal diffusivity measurement uncertainty is given by the square root of the first diagonal element of C_m multiplied by a coverage factor of 2. This coverage factor is derived, under the Gaussian noise hypothesis, from the Student distribution with a number of degrees of freedom of $N-4$, typically 9996, and a confidence level of 95% [8].

4. EXPERIMENTAL RESULTS

The thermal diffusivities of platinum, germanium, titanium, and copper have been measured. Each sample was placed in a tube furnace and heated in air to 900 K. In the case of titanium and copper, an oxide layer formed on the surface. The sample temperature was controlled by a sheathed Type K thermocouple positioned 5 mm below the sample front surface. The accuracy of the temperature measurement was about ± 2 K,

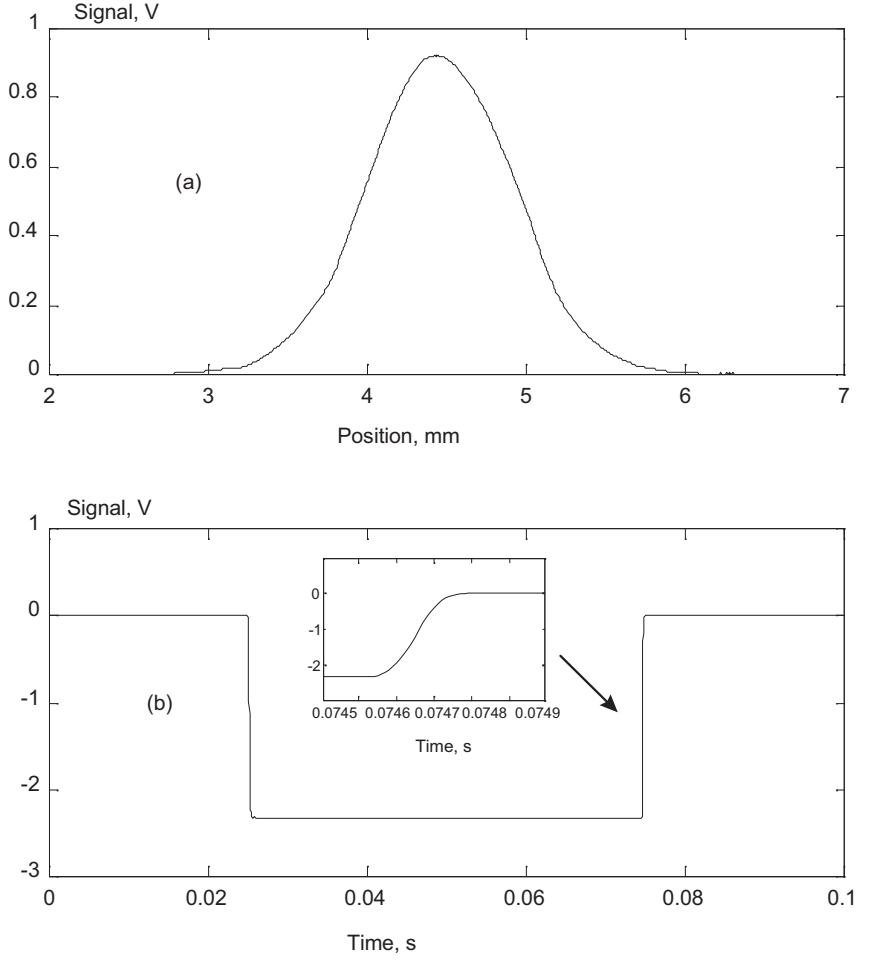

Fig. 3. Boundary conditions measured for the analysis of platinum. (a) Beam profile. (b) Laser intensity time dependence. The inset shows the finite rise time of the laser excitation (~ 0.2 ms).

a range in which no significant variation of the thermal diffusivity was expected for the samples under investigation. A beam diameter of about 2 mm and a scanning frequency of 10 Hz were used. The measured boundary conditions for the platinum sample are shown in Fig. 3. The laser power was set at about 100 mW in order to minimize nonlinear effects in the thermal radiance signal. A temperature perturbation of about 2 K was induced in the samples. To compensate for the very low corresponding infrared signal level, a large number of periods, typically 1000, were

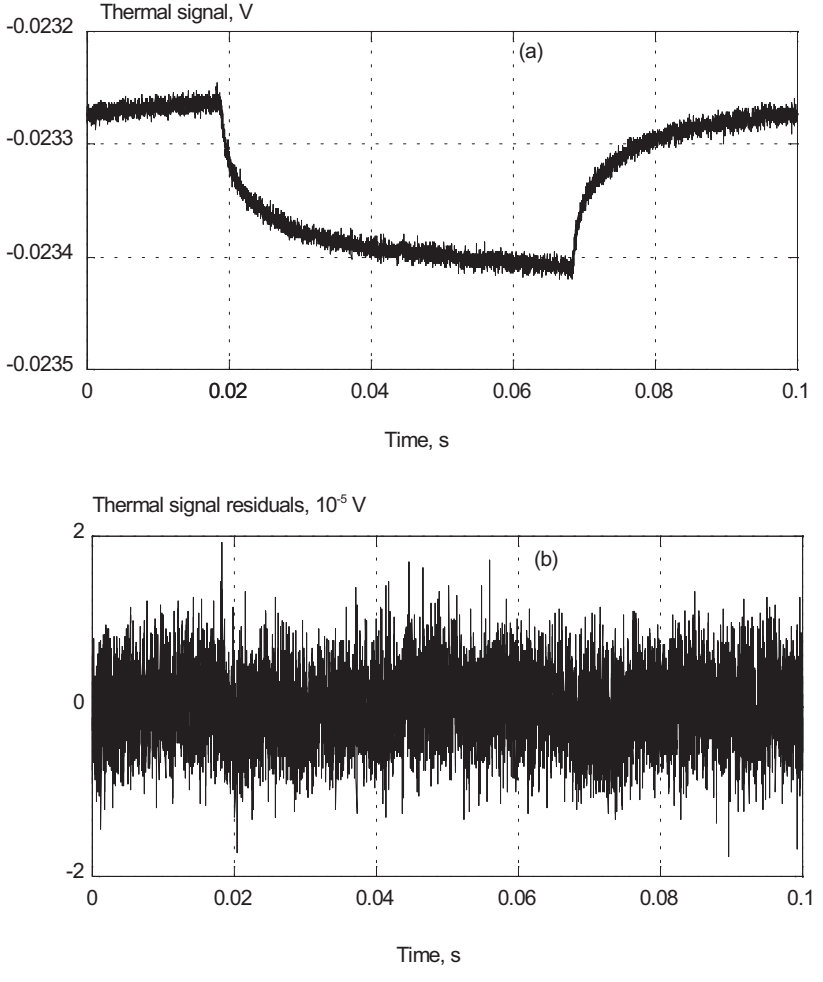

Fig. 4. Thermal radiance signal measured for platinum. (a) Experimental data (noisy signal) and best fit (continuous line). (b) Data residuals after fitting.

Table I. Experimental Results on the Thermal Diffusivity of Pure Metals

Material	Purity (mass%)	T (K)	Surface state	This work • thermal diffusivity • standard deviation • 95% conf. interval ($m^2 \cdot s^{-1}$)	Literature [9] • thermal diffusivity • uncertainty • conf. interval ($m^2 \cdot s^{-1}$)
platinum	99.99	900	polished no oxide layer	$D = 2.56 \times 10^{-5}$ $\sigma = 2 \times 10^{-7}$ $[2.52; 2.60] \times 10^{-5}$	$D = 2.46 \times 10^{-5}$ $\pm 8\%$ $[2.3; 2.7] \times 10^{-5}$
titanium	99.6	800	polished transparent oxide layer	$D = 6.43 \times 10^{-6}$ $\sigma = 4 \times 10^{-8}$ $[6.35; 6.51] \times 10^{-6}$	$D = 6.99 \times 10^{-6}$ $\pm 10\%$ $[6.3; 7.7] \times 10^{-5}$
germanium	99.999	900	unpolished no oxide layer	$D = 8.70 \times 10^{-6}$ $\sigma = 7 \times 10^{-8}$ $[8.56; 8.84] \times 10^{-6}$	$D = 9.00 \times 10^{-6}$ $\pm 13\%$ $[7.8; 10.2] \times 10^{-6}$
copper	unknown	900	polished black oxide layer	$D = 8.9 \times 10^{-5}$ $\sigma = 2 \times 10^{-6}$ $[8.5; 9.3] \times 10^{-5}$	$D = 9.35 \times 10^{-5}$ $\pm 6\%$ $[8.8; 9.9] \times 10^{-5}$

averaged according to the procedure described in Section 2. The thermal radiance signal measured on platinum and the best fit are shown in Fig. 4. Table I presents the results obtained with the set of samples. The thermal diffusivities of platinum, titanium, and germanium were measured with an uncertainty of about $\pm 1.5\%$, calculated according to the procedure described in Section 3. These results are in good agreement with literature values [9]. Platinum, germanium, and titanium gave excellent agreement between experimental data and theoretical predictions. The histogram of the fitting residuals revealed a nearly perfect Gaussian distribution, which validates the Gaussian noise hypothesis used for expressing the measurement uncertainties. In contrast, the data collected with copper showed residual peaks after the fitting procedure. In this case, the homogeneous model for the sample is almost certainly not appropriate because of the thick black oxide layer formed at high temperature in air.

5. CONCLUSIONS

By accurately measuring the boundary conditions associated with a laser-based thermal experiment, it has been demonstrated that the thermal diffusivity of solids can be measured with an uncertainty of about $\pm 1.5\%$. The results presented in this work concerned platinum, titanium, germanium, and copper. Although the uncertainties of the literature values are

not generally as good, they agree well with our measurements. However, the data obtained with copper showed that the technique does not give very good results when the surface oxidizes too much. A further validation of the technique would consist in measuring the thermal diffusivity of a very high purity sample in a controlled atmosphere as a function of temperature.

Using the linear system theory, it is theoretically possible to perform the measurement of the thermal diffusivity by adaptive filtering. Such a filter could be implemented on a digital electronic circuit allowing the experimental setup to determine the thermal diffusivity in real time.

REFERENCES

1. G. J. Edwards and A. P. Levick, *Proc. 7th Int. Symp. Temp. Thermal Measurements Ind. Sci. TEMPMEKO'99* (Imeko/Nmi Van Swinden Laboratorium, Delft, 1999), p. 619.
2. W. J. Parker, R. J. Jenkins, C. P. Butler, and G. L. Abbott, *J. Appl. Phys.* **32**:1679 (1961).
3. B. Remy, D. Maillet, and S. André, *Int. J. Thermophys.* **19**:951 (1998).
4. H. G. Walther and T. Kitzing, *J. Appl. Phys.* **84**:1163 (1998).
5. P. E. Nordal and S. O. Kanstad, *Phys. Scr.* **20**:659 (1979).
6. H. S. Carslaw and J. C. Jaeger, *Conduction of Heat in Solids*, 2nd Ed. (Oxford University Press, Oxford, 1959).
7. M. N. Ösizik, *Heat Conduction*, 2nd Ed. (Wiley, New York, 1993).
8. J. V. Beck and K. J. Arnold, *Parameter Estimation in Engineering and Science* (Wiley, New York, 1977).
9. Y. S. Touloukian, R. K. Kirby, R. E. Taylor, and T. Y. R. Lee, eds., *Thermophysical Properties of Matter* (IFI/Plenum, New York, 1972), Vol. 10.

Printed in Belgium